

# Run plan for $^{24}\text{Mg}+\alpha$ measurements at Novae energies

August 27, 2018

## 1 Introduction

The modeling of novae light curves provides a ready test for our understanding of the dynamics of stars and the underlying nuclear processes that drive them. Due to the high temperatures reached in a novae, in the 1 to 2 GK range, many reactions can participate in the energy generated and nuclei that are created. A recent sensitivity study by [7] notes that while the  $^{24}\text{Mg}(\alpha, p)^{27}\text{Al}$  reaction does not have a significant effect on nucleosynthesis in such an environment, it may have an impact on the overall energy generation and therefore the observed light curve. For temperature ranges of 1 to 2 GK, the corresponding  $\alpha$ -particle beam energies of interest range from 1 to 4 MeV.

Direct measurements of the  $^{24}\text{Mg}(\alpha, p)^{27}\text{Al}$  reaction are limited to [2]. In this seminal work, not only was the  $^{24}\text{Mg}(\alpha, p)^{27}\text{Al}$  reaction measured but also the  $^{24}\text{Mg}(\alpha, \alpha)^{24}\text{Mg}$ ,  $^{27}\text{Al}(p, \alpha)^{24}\text{Mg}$  and the  $^{27}\text{Al}(p, p)^{27}\text{Al}$  reactions over the same excitation energy range in the  $^{28}\text{Si}$  compound. In addition, resonances that were populated in all reaction were highlighted. However, this early data lacks absolute scale and were only investigated at one angle. Further measurements have been made of the  $^{24}\text{Mg}(\alpha, \alpha)^{24}\text{Mg}$  reaction by [9, 1]. More attention has been paid to the  $^{24}\text{Mg}(\alpha, \gamma)^{28}\text{Si}$  reaction as its inverse reaction plays a role in silicon burning in massive stars [3, 4, 8]. Measurements of these reactions give helpful information of the location of possible  $(\alpha, p)$  resonances, but often only the capture strength  $\omega\gamma_{(\alpha, \gamma)}$  is known so the contributions from the corresponding levels to the  $(\alpha, p)$  reaction remains unknown.

As a self-conjugate nuclear reaction,  $^{24}\text{Mg}+\alpha$  reactions has been measured at higher energies in order to study the  $\alpha$ -cluster nature of the reaction.

As a final note, the  $^{24}\text{Mg}+\alpha$  reactions can be studied at higher energies of about  $E_\alpha \approx 10$  MeV as an indirect way of probing the astrophysically important  $^{12}\text{C}+^{16}\text{O}$  reaction.

Most of the information for calculating the  $^{24}\text{Mg}(\alpha, p)^{27}\text{Al}$  reaction comes from a high precision measurement of the inverse reaction [6, 5]. Scattering and inelastic scattering cross sections for the  $^{27}\text{Al}(p, p_0)^{27}\text{Al}$ ,  $^{27}\text{Al}(p, p_1)^{27}\text{Al}$ , and  $^{27}\text{Al}(p, p_1)^{27}\text{Al}$  were also measured concurrently as well as the  $^{27}\text{Al}(p, \alpha_1)^{24}\text{Mg}$  reaction. An extensive  $R$ -matrix analysis was performed, extracting the partial

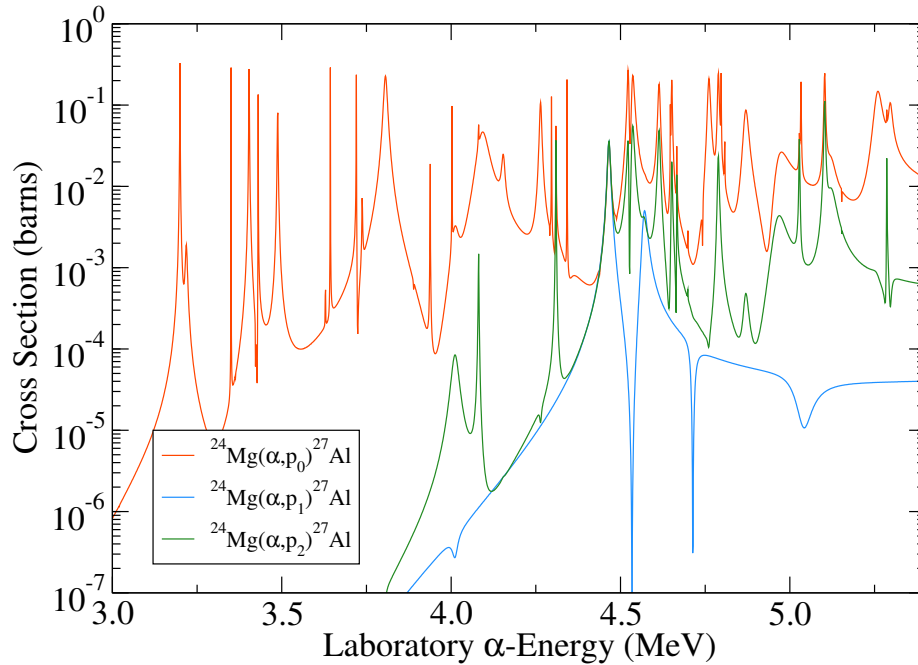


Figure 1: Estimate of the  $^{24}\text{Mg}(\alpha, p_0)^{27}\text{Al}$ ,  $^{24}\text{Mg}(\alpha, p_1)^{27}\text{Al}$ , and  $^{24}\text{Mg}(\alpha, p_2)^{27}\text{Al}$  reactions from measurements of the inverse  $^{27}\text{Al}+p$  reactions by [6, 5].

widths for the many resonances that were observed. Since all of the decay partial widths are known the cross sections can be calculated for not only the  $^{24}\text{Mg}(\alpha, p_0)^{27}\text{Al}$  reaction but also for the  $^{24}\text{Mg}(\alpha, p_1)^{27}\text{Al}$  and  $^{24}\text{Mg}(\alpha, p_2)^{27}\text{Al}$  reactions that play a role at higher energies. An estimate of the cross sections of interest is given in Fig. 1 via an  $R$ -matrix calculation with the code AZURE2.

## 2 Setup

The experiment will be performed using the 10 MV Tandem Pelletron accelerator and will cover the range from 5.4 MeV  $\alpha$ -particle energy down to as low as can be reached. The low energy limit will depend on how low in energy a bunched  $^4\text{He}^{++}$  beam can be produced with sufficient intensity ( $> \text{a few } 10^7 \text{ s of nA}$ ). From previous runs this should certainly be down to 4 MeV, but may also be able to be pushed lower. The beam will be impinged on thin transmission targets positioned at the center of the “R2D2” scattering chamber in the east target room. An array of 15 photodiodes will act as charged particle detectors for  $\alpha$ -particles and protons that will react with the thin targets. The detectors are placed at approximately 23.5 cm from the target and have double collima-

tion, the smallest of which is 0.25 inches. The detectors cover an angular range from 70 to 165° mostly in 5° increments. Targets are made by evaporating a thin film of pure, isotopically enriched  $^{24}\text{Mg}$  (99.91(1)%) onto a thin carbon (natural abundance) backing (20(2)  $\mu\text{g}/\text{cm}^2$ ). The thickness of enriched  $^{24}\text{Mg}$  targets that were produced range from 5 to 20  $\mu\text{g}/\text{cm}^2$ . Thin targets are essential because of the close spacing of the narrow levels that dominate much of the cross section.

The R2D2 target ladder is adjustable and can be loaded with up to seven different targets. Khachatour has prepared Mg targets as described above. The targets will definitely oxidize to some degree. The degree of oxidization can be determined by comparison of the  $^{16}\text{O}(\alpha, \alpha)^{16}\text{O}$  scattering yield to that of the  $^{24}\text{Mg}(\alpha, \alpha)^{24}\text{Mg}$  scattering yield and the known cross sections for both. Oxygen will also be present in the carbon backing so the contribution from this source must be subtracted by doing background runs with a carbon blank. In order to obtain an absolute efficiency,  $\alpha$ -scattering from a thin gold target will also be observed at a few energies. The high  $Z$  of the gold targets ensures that the cross section will be dominated by Rutherford scattering at these low energies.

The targets that will be used will be:

1. Gold, 200  $\mu\text{g}/\text{cm}^2$
2. Carbon, 20  $\mu\text{g}/\text{cm}^2$
3. Carbon, 20  $\mu\text{g}/\text{cm}^2$
4.  $^{24}\text{Mg}$ , 5  $\mu\text{g}/\text{cm}^2$
5.  $^{24}\text{Mg}$ , 5  $\mu\text{g}/\text{cm}^2$
6.  $^{24}\text{Mg}$ , 10  $\mu\text{g}/\text{cm}^2$
7.  $^{24}\text{Mg}$ , 20  $\mu\text{g}/\text{cm}^2$

In order to cleanly separate  $\alpha$ -particles from protons, the time-of-flight technique will also be utilized. This will be very helpful because the kinematics at these energies is such that at several energies and angles the  $^{12}\text{C}(\alpha, \alpha_0)^{12}\text{C}$  peak will mask the  $^{24}\text{Mg}(\alpha, p_0)^{27}\text{Al}$  peak. Since the yield from the  $^{24}\text{Mg}(\alpha, p_0)^{27}\text{Al}$  will be 2 to 3 orders of magnitude smaller than that from  $^{12}\text{C}(\alpha, \alpha_0)^{12}\text{C}$ , it is highly desirable to have a way to more cleanly distinguish the particles. One could also think of perhaps using  $E - \Delta E$  detectors but these would need to be very thin because of the low particle energies, we don't have many of them, and they would complicate the electronics setup significantly. In addition, at forward angles the recoil peaks will be observed and these may also overlap with the proton peaks.

We will use a bunched beam of  $^4\text{He}^{++}$ . The bunching system can produce a bunched beam with a timing resolution of about 2 ns. For the most extreme case, at 5.4 MeV and 50°, the time for a proton from the  $^{24}\text{Mg}(\alpha, p_0)^{27}\text{Al}$  reaction to get from the target to the detector ( $d = 23.5$  cm) will be 9.4 ns while an  $\alpha$  particle from the  $^{12}\text{C}(\alpha, \alpha_0)^{12}\text{C}$  will take 16.4 ns. This should be sufficient time for clean separation. The bunching repetition rate will be XXX ns.

### 3 Run Plan

The overall run plan will be:

1. Efficiency and detector calibrations
2. Main running (thick target)
3. Main running (thin target)
4. Carbon background runs

#### 3.1 Efficiency and energy calibration and gain and threshold fine tuning

The first step in the running will be to calibrate the efficiency and the energy scale of the detectors. To do this, we will use  $\alpha$  scattering off of gold. At the energies of this experiment the cross section is Rutherford to high precision for this high  $Z$  reaction, even at backward angles. At least two energies should be done, probably at  $E_\alpha = 4$  and 5 MeV in order to get two points for the energy calibration of the detectors.

In addition, while we will have done some adjustments of the thresholds and gains of the detectors using the mixed  $\alpha$ -source during the setup. Time should be spent to refine these settings so that they are optimized for the remainder of the experiment.

**Note:** Be very careful of the beam intensity during this part. If too much beam is used you can easily burn up the forward angle detectors because the target is relatively thick and the cross section changes very rapidly as a function of angle for this high  $Z$  reaction. Probably want only a couple nano-amps.

#### 3.2 Main experimental running

We will start the experiment at  $E_\alpha = 5.4$  MeV and take fine energy steps down to as low as we can go and still get reasonable beam intensity. The energy steps will be dictated by how fast the cross section is changing as a function of energy. The cross section is dominated by strong narrow resonances over much of the energy range, so we will likely spend most of the time doing careful scans of these resonances. We will use our thin target ( $5 \mu\text{g}/\text{cm}^2$ ) in regions where the yields allow in order to obtain an excitation curve that is as close to a cross section as we can get over as much of the energy range as possible. However, to get a rough mapping of the cross section, it will be better to first go over the range of interest with the thick target for faster runs.

So we will do:

1. Scan of excitation curve from  $E_\alpha = 5.4$  MeV down to lowest energy with thick target of  $20 \mu\text{g}/\text{cm}^2$

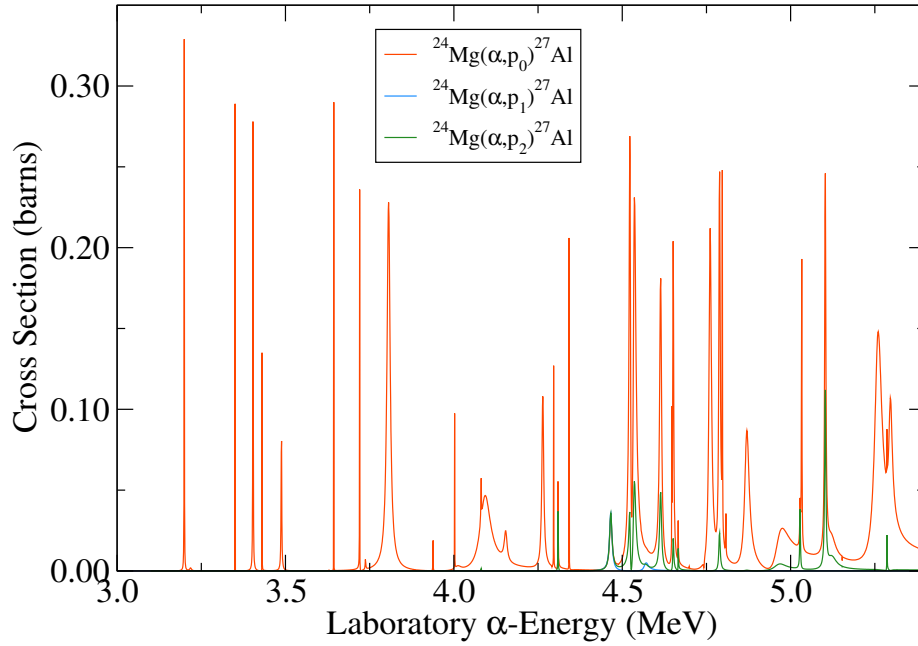


Figure 2: Estimate of the  $^{24}\text{Mg}(\alpha, p_0)^{27}\text{Al}$ ,  $^{24}\text{Mg}(\alpha, p_1)^{27}\text{Al}$ , and  $^{24}\text{Mg}(\alpha, p_2)^{27}\text{Al}$  reactions from measurements of the inverse  $^{27}\text{Al}+p$  reactions by [6, 5].

2. Repeat excitation curve scan with  $5 \mu\text{g}/\text{cm}^2$  thick target if time allows

Over nearly the entire excitation energy range the  $^{24}\text{Mg}(\alpha, p)^{27}\text{Al}$  cross section is dominated by the  $^{24}\text{Mg}(\alpha, p_0)^{27}\text{Al}$  branch. Only over a few isolated resonances are the excited state transitions expected to compete. This can be seen more clearly in a linear scale plot of Fig. 1, as shown in Fig. 2.

### 3.3 Carbon background runs

After completion of the standard excitation curve runs, carbon backing background runs will be done for each energy that was done in the Main experimental runs. The exception to this is over regions where thick target yield curves are being scanned. Here the energy steps are very small and the yields are constant, so only one background run needs to be done for each thick target plateau region. In addition, for the carbon background runs, ToF is not necessary since only  $\alpha$  particles will be produced.

## References

- [1] J. Cseh, E. Koltay, Z. Máté, E. Somorjai, and L. Zolnai. Levels of  $^{28}\text{Si}$  from the  $^{24}\text{Mg}(\alpha, \alpha)^{24}\text{Mg}$  and  $^{24}\text{Mg}(\alpha, \gamma)^{28}\text{Si}$  reactions. *Nucl. Phys. A*, 385(1):43–56, aug 1982.
- [2] S. G. Kaufmann, E. Goldberg, L. J. Koester, and F. P. Mooring. Energy Levels in  $\text{Si}^{28}$  Excited by Alpha-Particles on  $\text{Mg}^{24}$ . *Phys. Rev.*, 88(3):673–676, nov 1952.
- [3] P. Lyons. Total yield measurements in  $^{24}\text{Mg}(\alpha, \gamma)^{28}\text{Si}$ . *Nucl. Phys. A*, 130(1):25–30, jun 1969.
- [4] J. Maas, E. Somorjai, H. Graber, C. Van Den Wijngaart, C. Van Der Leun, and P. Endt. Investigation of  $^{28}\text{Si}$  levels with the  $(\alpha, \gamma)$  and  $(p, \gamma)$  reactions. *Nucl. Phys. A*, 301(2):213–236, may 1978.
- [5] R. O. Nelson, E. G. Bilpuch, C. R. Westerfeldt, and G. E. Michell. Proton resonances in  $^{28}\text{Si}$  from  $E_x = 13.4$  to 14.5 MeV. *Phys. Rev. C*, 30:755–764, Sep 1984.
- [6] R. O. Nelson, E. G. Bilpuch, C. R. Westerfeldt, and G. E. Mitchell. Proton resonances in  $^{28}\text{Si}$  from  $E_x = 12.5$  to 13.4 MeV. *Phys. Rev. C*, 29(5):1656–1663, may 1984.
- [7] A. Parikh, J. José, F. Moreno, and C. Iliadis. The Effects of Variations in Nuclear Processes on Type I X-Ray Burst Nucleosynthesis. *Astrophys. J. Suppl. Ser.*, 178(1):110–136, sep 2008.
- [8] E. Strandberg, M. Beard, M. Couder, A. Couture, S. Falahat, J. Görres, P. J. LeBlanc, H. Y. Lee, S. O’Brien, A. Palumbo, E. Stech, W. P. Tan, C. Ugalde, M. Wiescher, H. Costantini, K. Scheller, M. Pignatari, R. Azuma, and L. Buchmann.  $^{24}\text{Mg}(\alpha, \gamma)^{28}\text{Si}$  resonance parameters at low  $\alpha$ -particle energies. *Phys. Rev. C*, 77(5):055801, may 2008.
- [9] J. A. Weinman, L. Meyer-Schützmeister, and L. L. Lee. States in  $^{28}\text{Si}$  with  $12.7 < E_x < 13.7$  MeV by  $(\alpha, \gamma)$  and  $(\alpha, \alpha)$  Reactions on  $^{24}\text{Mg}$ . *Phys. Rev.*, 133(3B):B590–B597, feb 1964.